Properties of [N,N′-di(n-propyl)-4,4′-bipyridylium]$^{2+}$ (7,7,8,8,-Tetracyanoquinodimethane)$_4^{2-}$

G. J. Ashwell†, I. Diaconu*, D. D. Eley, S. C. Wallwork, and M. R. Willis
Department of Chemistry, University of Nottingham, Nottingham, NG7 2RD, U.K.

Z. Naturforsch. **34a**, 1–5 (1979); received May 3, 1978

Dedicated to Professor Dr. G.-M. Schwab on his 80th Birthday

The crystal structure and electrical properties of [*N*,*N*′-di(n-propyl)-4,4′-bipyridylium]$^{2+}$-(7,7,8,8-tetracyanoquinodimethane)$_4^{2-}$, (DPrBP)$^{2+}$(TCNQ)$_4^{2-}$, are reported. The complex is monoclinic with the space group $P2_1/c$ and lattice constants $a = 13.334(1)$, $b = 25.954(3)$, $c = 7.877(1)$ Å, $\beta = 93.66°$, $Z = 2$. The single crystal dc resistivities at 300 K along a, b and c are 3300, 200 and 800 Ω cm respectively with activation energies of 0.36, 0.22 and 0.30 eV. The existence of a hopping mechanism in addition to a frequency independent conduction process is indicated by a.c. conductivity data obtained on a compressed disc between 10 and 10^5 Hz.

Introduction

The crystal structures of the majority of TCNQ salts are characterised by a series of parallel linear stacks of overlapping TCNQ molecules. Such an arrangement gives rise to anisotropy which has been observed for conductivity [1], Hall mobility [2] and thermoelectric emf [3]. The anisotropic conductivity is generally such that the direction of highest conductivity is parallel to the TCNQ stack. The activation energies for conduction in such anisotropic media, however, are often remarkedly isotropic.

In bipyridylium-TCNQ salts [4–10] the TCNQ's are arranged plane-to-plane in columns within two-dimensional arrays separated along a third axis by the cations. Strong coupling between adjacent columns, as indicated by short inter-molecular contacts of ~3.3 Å, generally results in nearly isotropic conductivities within the array and a lower conductivity perpendicular to it. In this paper the crystal structure and electrical conductivity of (DPrBP)$^{2+}$(TCNQ)$_4^{2-}$ are reported. Although the structure is very similar to that of the related complex (DEBP)$^{2+}$(TCNQ)$_4^{2-}$ [4] the electrical properties show differences which may reflect crystal imperfections.

Experimental

Preparation of (DPrBP)$^{2+}$(TCNQ)$_4^{2-}$

To a hot acetonitrile solution (200 ml) of TCNQ (0.5 g) was added on aqueous solution (10 ml) of *N*,*N*′-di(n-propyl)-4,4′-bipyridylium diiodide (0.2 g) and the resulting solution allowed to cool slowly. After 48 hours the complex (0.2 g) was collected and washed with toluene and ether to remove unreacted neutral TCNQ. Black parallelpiped crystals of (DPrBP)$^{2+}$(TCNQ)$_4^{2-}$ were obtained and analysed by elemental, spectroscopic and crystallographic methods.

	C	H	N	$\varepsilon_{395}/\varepsilon_{842}$
Calculated	72.59	3.59	23.82	2.2
Found	72.73	3.5	24.32	2.5

The discrepancy between the calculated and experimental ratios of the molar extinction coefficient at 395 and 842 nm is probably due to the instability of the complex. In acetonitrile (DPrBP)$^{2+}$(TCNQ)$_4^{2-}$ readily decomposes to the charge transfer complex 4,4′-bipyridyl(TCNQ)$_2$. However, crystallographic determination of the unit cell volume, (2720 Å^3) and a density measurement by flotation, (1.29 g cm^{-3}) confirmed the stoichiometry as (DPrBP)$^{2+}$(TCNQ)$_4^{2-}$.

Structure Determination

The space group and unit cell dimensions were obtained initially from oscillation and Weissenberg photographs using Cu$K\alpha$ radiation. The cell constants were subsequently refined on a Hilger and Watts computer-controlled, four-circle diffractometer. Intensity data were collected on the diffractometer using a $\Theta/2\Theta$ scan, a scintillation counter and Mo$K\alpha$ radiation. The intensities were corrected for Lorentz and polarisation factors but not for absorption. The structure was solved from

† Present address: Department of Chemistry, Sheffield City Polytechnic, Pond Street, Sheffield SI IWG, England.

* Present address: P. Poni, Institute of Macromolecular Chemistry, Jassy, Romania.

a three-dimensional Patterson synthesis and refined by a block-diagonal least-squares method to $R = 0.070$ using 3277 significant reflections.

Sample Preparation and Electrical Measurement

150 mg samples of $(DPrBP)^{2+}(TCNQ)_4^{2-}$ were finely ground and compressed for two minutes at 75 MPa in an evacuated die. Compacted pellets and single crystals were mounted on fine copper wire using Acheson 915 Electrodag (high conductivity silver paint) as electrodes and degassed at 350 K for sixteen hours under vacuum. DC conductivities were determined by a two-probe technique. The contact resistance and lead resistance were negligible relative to those of the pellets and crystals. AC measurements, conductivity and capacitance, were made on compacted pellets in the range 10 to 10^5 Hz using a General Radio 1621 bridge.

Results and Discussion

Description of the Structure

$(DPrBP)^{2+}(TCNQ)_4^{2-}$ and the ethyl analogue [4] $(DEBP)^{2+}(TCNQ)_4^{2-}$ are very nearly isostructural. Within each the TCNQ molecules are stacked plane-to-plane in groups of four along *b* with no direct overlap between tetrads. This gives rise to a series of two-dimensional arrays of TCNQ molecules parallel to the (100) plane separated by bipyridylium cations (Figure 1). Within tetrads the overlaps TCNQ(A)-TCNQ(A′) and TCNQ(A)-TCNQ(B) are virtually identical and similar to those found in the majority of complexes where the exocyclic double bond of one molecule is situated directly above the ring of the second. This staggering is in a consistent direction throughout each tetrad (Fig. 2), a feature also found in the structures of the related methyl and benzyl complexes $(DMBP)^{2+}(TCNQ)_3^{2-}$ and $(DBzBP)^{2+}(TCNQ)_4^{2-}$. In $(DPrBP)^{2+}(TCNQ)_4^{2-}$ the perpendicular inter-TCNQ separations within tetrads are 3.20 Å (AA′) and 3.23 Å (AB).

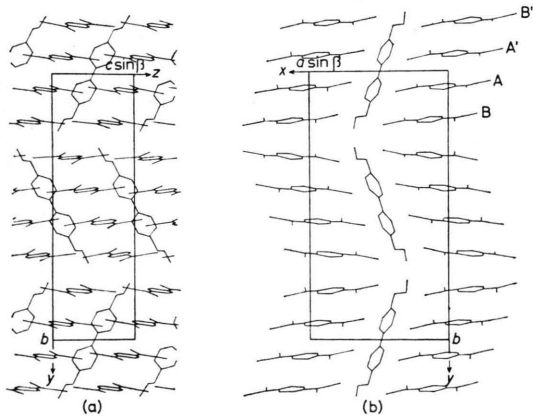

Fig. 1. Crystal structure of $(DPrBP)^{2+}(TCNQ)_4^{2-}$ projected (a) along *a* and (b) along *c*.

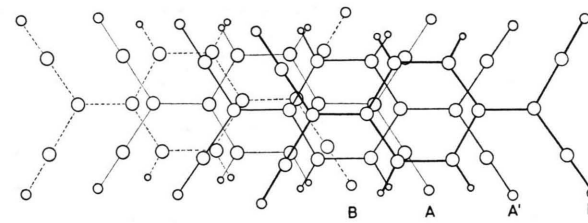

Fig. 2. Quinonoid double bond to aromatic ring overlap with the molecular staggering in a consistent direction throughout the tetrad.

DC Electrical Properties

$(DPrBP)^{2+}(TCNQ)_4^{2-}$ crystallises as monoclinic parallelpiped plates with *c* along the length, *a* across the width and *b* perpendicular to the plate. At 300 K the resistivities along *a*, *b* and *c* are 3300, 200 and 800 Ω cm respectively. Within the TCNQ array, i.e. along *b* and *c*, similar values reflect the two-dimensionality, not normally observed in TCNQ complexes but common to bipyridylium-TCNQ salts. Along *a* the lower conductivity is consistent with the greater separation between TCNQ's and the periodic change in potential. The activation energies for conduction *E* (in $\sigma = \sigma_0 e^{-E/kT}$) corresponding to the *a*, *b* and *c* axes are 0.36, 0.22 and 0.30 eV respectively. Due to crystal fracture these values were obtained for only a limited temperature range (273 to 400 K) but were reproducible for several crystals studied. The electrical properties of the compacted pellet (750 Ω cm at 300 K, activation energy 0.22 eV) mainly reflect the high conductivity direction of the single crystal.

The similarity of the molecular and crystal structures of $(DEBP)^{2+}(TCNQ)_4^{2-}$ and $(DPrBP)^{2+}$-$(TCNQ)_4^{2-}$, which are compared in Table 1, makes a comparison of their electrical properties of particular significance. Similar electrical behaviour would suggest that intrinsic properties are dominant whereas differences would suggest either an

Table 1. Comparison of the structural and electrical properties of $(DEBP)^{2+}(TCNQ)_4^{2-}$ and $(DPrBP)^{2+}(TCNQ)_4^{2-}$. * Denotes the shortest contact between non-overlapping tetrads along *b*.

	$(DEBP)^{2+}$ $(TCNQ)_4^{2-}$	$(DPrBP)^{2+}$ $(TCNQ)_4^{2-}$
Perpendicular separation (Å)		
TCNQ(A)–TCNQ(A′)	3.16	3.20
TCNQ(A)–TCNQ(B)	3.22	3.23
TCNQ(B)–TCNQ(B′)	3.32 *	3.46 *
Dihedral angles (°)		
TCNQ(A)–TCNQ(B)	2.8	1.3
TCNQ(B)–TCNQ(B′)	16.6	21.1
TCNQ(A)–cation	60.5	61.5
TCNQ(B)–cation	60.5	60.9
Electrical properties		
a axis	8300 Ω cm	3300 Ω cm
	0.25 eV	0.36 eV
b axis	400 Ω cm	200 Ω cm
	0.28 eV	0.22 eV
c axis	310 Ω cm	800 Ω cm
	0.27 eV	0.30 eV

unexpected degree of structure sensitivity or that impurities or defects are involved.

The single crystal conductivities at 300 K of $(DEBP)^{2+}(TCNQ)_4^{2-}$ and $(DPrBP)^{2+}(TCNQ)_4^{2-}$ (Table 1) are somewhat similar in magnitude and anisotropy supporting the idea [4] of a two-dimensional band structure associated with the sheets of TCNQ's. The activation energies along *a*, *b* and *c* $(DEBP)^{2+}(TCNQ)_4^{2-}$ are within experimental error isotropic suggesting a band gap of ~ 0.5 eV. In contrast those of $(DPrBP)^{2+}(TCNQ)_4^{2-}$ are anisotropic. Whilst the values for the *b* and *c* axes are just within experimental error of the activation energies obtained for $(DEBP)^{2+}(TCNQ)_4^{2-}$ the value for the *a* axis is significantly higher. A similar effect has been observed [6] in [1,2-di(*N*-ethyl-4-pyridinium)ethylene]$^{2+}(TCNQ)_4^{2-}$ for $T > 270$ K. A polaron mechanism for conduction between TCNQ sheets is a possibility but the absence of the effect in $(DEBP)^{2+}(TCNQ)_4^{2-}$ and several similar materials suggests extrinsic behaviour.

There are three explanations for the anisotropy observed. (1) The activation energies were measured over a relatively short temperature range and may be subject to error arising from an anisotropic temperature dependence of the pre-exponential factor. (2) Crystal imperfections may give rise to the higher values along the non-stacking axes. (3) The properties are dependent upon minor variations in overlap and contact distances within the structures.

AC Electrical Properties

The frequency dependence of the conductivity (σ) of a polycrystalline specimen measured by the a.c. bridge technique is shown in Figure 3. It is clear that at higher temperatures and low frequency the conductivity is frequency independent, but at lower temperatures or higher frequencies the conductivity becomes frequency dependent. It is thus likely that the measured conductivity (σ) consists of a frequency independent component σ' and a frequency dependent component $\sigma(\omega)$.

$$\sigma = \sigma' + \sigma(\omega)\,. \tag{1}$$

The variation of σ, at different frequencies, as a function of reciprocal absolute temperatures is shown in Fig. 4 together with the d.c. conductivity. It is clear that at high temperatures the value of σ has the same value and same temperature dependence as $\sigma_{d.c.}$. This provides strong evidence that the frequency independent component σ' is in fact the d.c. conductivity. Furthermore, the agreement between σ' and $\sigma_{d.c.}$ indicates that slow polarisation processes such as can occur at electrodes are not

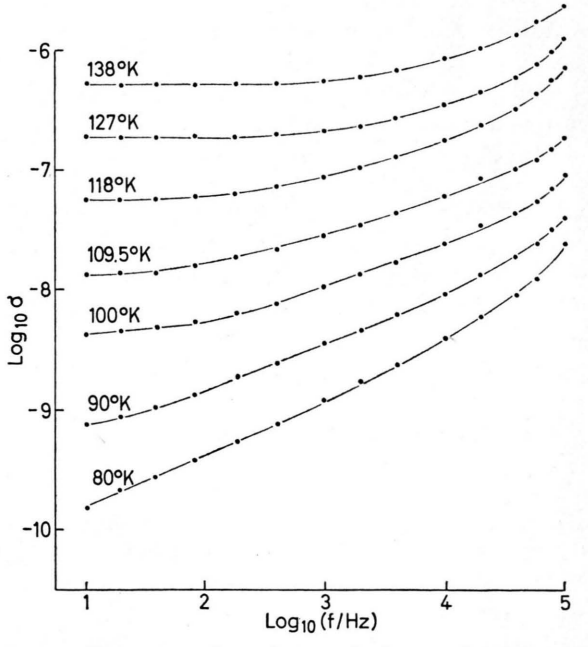

Fig. 3. Frequency dependence of the conductivity of $(DPrBP)^{2+}(TCNQ)_4^{2-}$.

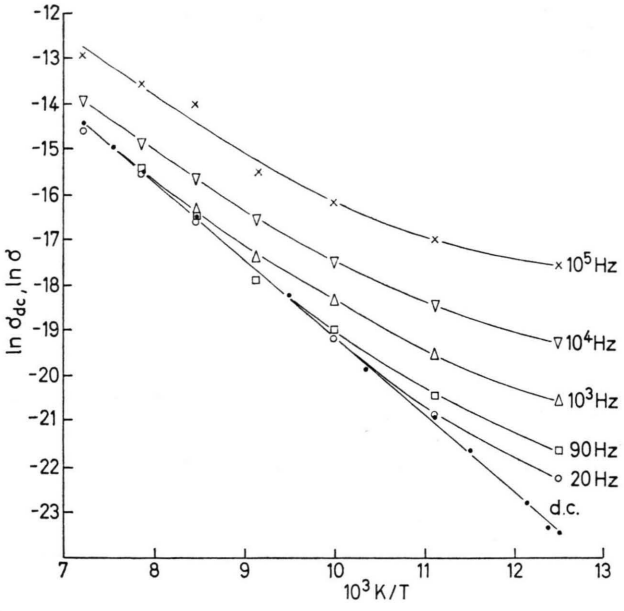

Fig. 4. Temperature dependence of the conductivity $(DPrBP)^{2+}(TCNQ)_4^{2-}$.

significant here and $\sigma_{d.c.}$ is a measure of the bulk conductivity.

The frequency dependent component $\sigma(\omega)$ is indicative of a.c. field assisted carrier hopping between localised sites. This type of loss has been studied by Pollak and Geballe [11], and Argall and Jonscher [12]. The frequency dependence is determined by the distribution of hopping centres. Hopping between identical pairs of localised sites at angular frequency, ω, gives

$$\sigma(\omega) \propto \omega^2/(\omega^2 + \Omega^2) \qquad (2)$$

where Ω is the natural frequency of hopping between the centres. (This is identical to the Debye factor involved in dipolar orientation and Maxwell-Wagner interfacial loss.) Thus at low frequencies ($\omega \ll \Omega$), $\sigma(\omega) \propto \omega^2$, but at high frequencies ($\omega \gg \Omega$), $\sigma(\omega) = \text{const}$. By averaging over for a completely random distribution of hopping centres the frequency dependence becomes

$$\sigma(\omega) \propto \omega^n \qquad (3)$$

where the value of n varies from 1 for single hops to 0.5 for multiple hops [13]. Substraction of $\sigma_{d.c.}$ from σ gives $\sigma(\omega)$ which is shown as a function of frequency in Figure 5. The low values of n may suggest that multiple hops are the dominant loss mechanism over most of the range studied, with

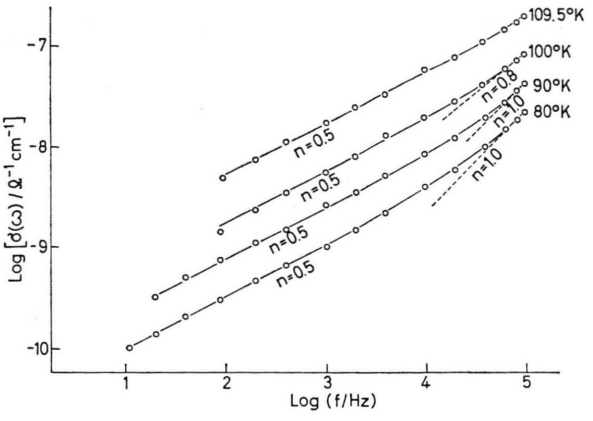

Fig. 5. Frequency dependence of $\sigma(\omega)$.

single hops becoming more significant at high frequencies. However, Jonscher's "screened- hopping" model can also give smaller values of n, in the range $0.5 < n < 0.8$, for hopping between only 2 equivalent sites.

The variation of sample capacitance with frequency is shown in Figure 6. The capacitance decreases steadily until a constant value is reached at high frequencies which is almost temperature independent. Now for a material in which $\sigma(\omega)$ varies as Eq. (3), the Kramers-Kronig relationship requires that the capacitance varies with frequency as

$$C = C_\infty + A\,\omega^{n-1}$$

where C and C_∞ are the equivalent parallel capacitance at frequency ω and infinite frequency

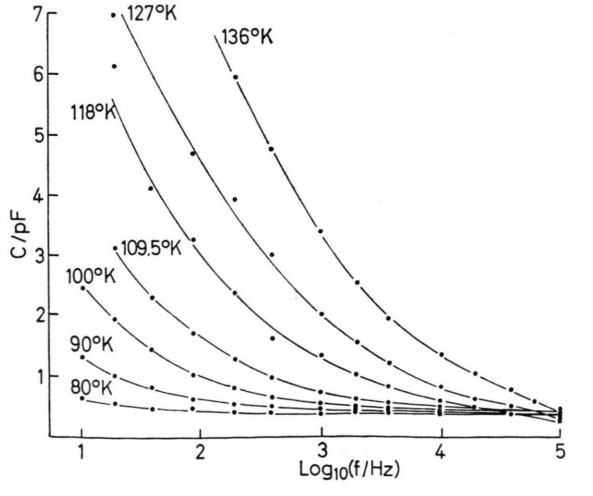

Fig. 6. Frequency dependence of the sample capacitance.

respectively, A is a constant and n is the exponent from Eq. (3). If C_∞ is taken as equal to the low temperature capacitance at 10^5 Hz, then $\log(C - C_\infty)$ vs. $\log \omega$ can be plotted (Figure 7). The values of n obtained from the slopes $(n - 1)$ agree well with those in Fig. 5, showing that the relationship is valid over most of the frequency range.

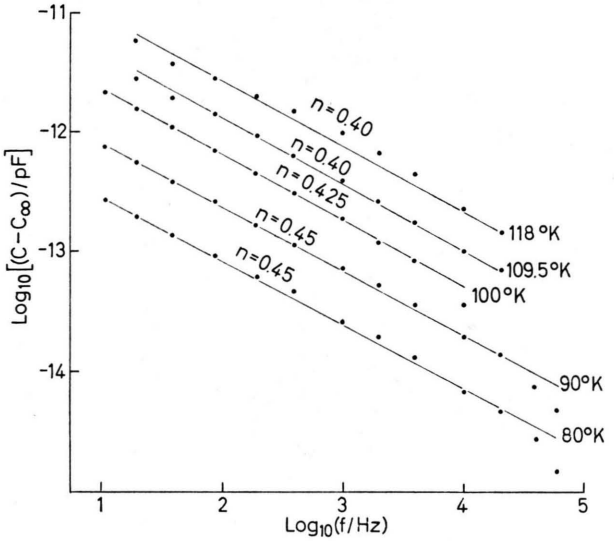

Fig. 7. Frequency dependence of $(C - C_\infty)$.

Conclusions

The d.c. conduction data of the present compound are closely similar to those for the structurally similar $(DEBP)^{2+}(TCNQ)_4^{2-}$, *N,N′*-diethyl-4,4′-bipyridylium]$^{2+}(TCNQ)_4^{2-}$, and in the latter case additional measurements of Seebeck coefficient allowed us to conclude that band theory was applicable in the plane (bc) of the TCNQ molecules [4]. Further, we may suppose the a.c. results are a property of the single crystal, not arising from intercrystalline defects, since we have found [15] similar a.c. behaviour for single crystals of the benzyl analogue $(DBzBP)^{2+}(TCNQ)_4^{2-}$. Since $\sigma(\omega) \to \sigma_{d.c.}$ as $\omega \to 0$ we must conclude the charge carriers active in d.c. are also responsible for the a.c. behaviour. The energy band is assumed to be two-dimensional, in the plane of the TCNQ's, with hopping as a possible mechanism for electron transport along the a axis across the cation plane [4]. The a.c. measurements may well pick out the a direction, but additionally there is the possibility of TCNQ vacancies which could give rise to localised electrons and two-site hopping in the b and c directions also. The strongly polarisable cations would be expected to give rise to strong screening of the carriers and therefore values of $n \to 0.5$ in $\sigma(\omega) \propto \omega^n$. Two site hopping would seem rather more probable than multiple hopping, sites, at least if these depend on presumably rather improbable multiple adjacent TCNQ vacancies. It is of great interest that Li-doped NiO shows similar behaviour [16], i.e. d.c. conduction plus Seebeck effect fitting band theory, while a.c. conductivity indicates hopping. However, in this case $\sigma(\omega)$ follows Eq. (2), corresponding to two equivalent unscreened sites, (Ni^{2+} and Ni^{3+} adjacent ions), as indeed might be expected for this relatively simple lattice.

Acknowledgements

The authors wish to thank Professor T. J. King for assistance with the diffractometry, the S.R.C. for contributing towards the cost of the diffractometer and the British Council for the award of a scholarship to I.D.

[1] W. J. Siemons, P. E. Bierstedt, and R. G. Kepler, J. Chem. Phys. **39**, 3523 (1963).
[2] J. P. Farges, A. Brau, D. Vasilescu, P. Dupuis, and J. Néel, Phys. Stat. Sol. **37**, 745 (1970).
[3] J. P. Farges and A. Brau, Phys. Stat. Sol. **64 B**, 269 (1974).
[4] G. J. Ashwell, D. D. Eley, S. C. Wallwork, and M. R. Willis, Proc. Roy. Soc. London A **343**, 461 (1975).
[5] G. J. Ashwell, S. C. Wallwork, S. R. Baker, and P. I. C. Berthier, Acta Cryst. **B 31**, 1174 (1975).
[6] G. J. Ashwell, D. D. Eley, R. J. Fleming, S. C. Wallwork, and M. R. Willis, Acta Cryst. **B 32**, 2948 (1976).
[7] G. J. Ashwell, D. D. Eley, S. C. Wallwork, M. R. Willis, G. D. Welch, and J. Woodward, Acta Cryst. **B 33**, 2252 (1977).
[8] G. J. Ashwell, D. D. Eley, A. Harper, A. C. Torrance, S. C. Wallwork, and M. R. Willis, Acta Cryst. **B 33**, 2258 (1977).
[9] G. J. Ashwell, D. D. Eley, N. J. Drew, S. C. Wallwork, and M. R. Willis, Acta Cryst. **B 33**, 2598 (1977).
[10] G. J. Ashwell, V. E. Bartlett, J. K. Davies, D. D. Eley, S. C. Wallwork, M. R. Willis, A. Harper, and A. C. Torrance, Acta Cryst. **B 33**, 2602 (1977).
[11] M. Pollak and T. H. Geballe, Phys. Rev. **122**, 1742 (1961).
[12] F. Argall and A. K Jonscher, Thin Solid Films **2**, 185 (1968).
[13] S. K. Bahl and K. L. Chopra, J. Appl. Phys. **41**, 2196 (1970).
[14] A. K. Jonscher, Phys. Stat. Sol. (b) **84**, 159 (1977).
[15] G. J. Ashwell, I. Diaconu, D. D. Eley, S. C. Wallwork, M. R. Willis, and J. Woodward, in preparation.
[16] S. Kabashima and T. Kawakubo, J. Phys. Soc. Japan **24**, 493 (1968).